EFFECT OF METAL OXIDE ADDITIONS TO V-BASED COMPLEX OXIDE CATALYSTS ON OXIDATIVE DEHYDROGENATION OF BUT-1-ENE

Naoki Ikenaga[1*], Junsuke Hatayama[1,2], and Kojiro Fuku[1]

(Received December 04, 2019)

Abstract

Buta-1,3-diene (BD), one of the most important products in the petrochemical industry, is mainly produced through the endothermic steam cracking of naphtha. Recently, the oxidative dehydrogenation (ODH) of n-butene (n-C_4H_8) has emerged as an attractive alternative due to the energy savings it offers. The ODH of n-C_4H_8 is reportedly improved by the addition of V-based complex oxide catalysts.

In this study, we added metal oxides to V-based complex oxide catalysts and examined the effects of this addition on the ODH of 1-C_4H_8. The addition of Mg and Co to the V-based complex oxides resulted in the highest BD yield of 22.5% with the lattice oxygen of the catalyst. Moreover, this catalyst also exhibited high ODH activity under an O_2 atmosphere.

1. Introduction

Buta-1,3-diene (BD) is an important intermediate product in the petrochemical industry. BD is a raw material used in synthesizing rubbers such as polybutadiene rubber and styrene-butadiene rubber [1]. BD is mainly produced through the purification of the C4 fraction, which is the main by-product in the production of ethylene by the steam cracking of naphtha. The steam cracking of naphtha, however, is associated with certain problems. One of these is that it is an endothermic reaction which cannot proceed expect under high temperatures of 700-800℃. Another problem with this process is that has relatively low BD selectivity.

An attractive alternative to the steam cracking of naphtha has recently emerged in the form of the oxidative dehydrogenation (ODH) of the C4 fraction (ODH of but-1-ene (1-C_4H_8); eq. (1)). This exothermic reaction can proceed at 400-500℃, a lower temperature than that required for the steam cracking of naphtha. Moreover, this process can produce BD more selectively. It has been reported that the Bi-Mo [2-4], Zn-Fe [5-7], and Fe-Sb [8] oxide catalysts have the high activity for the ODH of n-C_4H_8, yet the complete oxidation of the reactant and the products can proceed easily (eqs. (2), (3)).

$$C_4H_8 + 1/2O_2 \rightarrow C_4H_6 + H_2O \qquad \Delta H_{298.15} = -177\ \text{kJ/mol} \qquad (1)$$

$$C_4H_8 + 6O_2 \rightarrow 4CO_2 + 4H_2O \qquad \Delta H_{298.15} = -2717\ \text{kJ/mol} \qquad (2)$$

$$C_4H_6 + 11/2O_2 \rightarrow 4CO_2 + 3H_2O \qquad \Delta H_{298.15} = -2540\ \text{kJ/mol} \qquad (3)$$

1 Department of Chemical, Energy and Environmental Engineering, Kansai University, Suita, Osaka 564-8680, Japan

2 presently, UNITIKA LTD.

*Correspondence to: Naoki Ikenaga, Department of Chemical, Energy and Environmental Engineering, Kansai University, Suita, Osaka 564-8680. E-mail: ikenaga@kansai-u.ac.jp

In our laboratory, ODH of propane using the lattice oxygen of the VO_X/SiO_2 catalyst has been investigated as a means of preventing the complete oxidation of the substrates [9]. That study revealed that the lattice oxygen of V=O contributed to the high propylene yield. In addition, Kiyokawa, *et al.* have reported that the specific surface area and the lattice oxygen mobility of the catalyst can be promoted by adding Fe to the V-Mg catalyst [10]. On the other hand, the ODH of the C4 fraction is similar to the ODH of ethylbenzene in terms of the reaction mechanism. V/MgO catalyst shows high activity for the ODH of ethylbenzene with carbon dioxide because higher-valence V species are reduced to lower-valence V species during the dehydrogenation of ethylbenzene [11]. Furthermore, it has been reported that metal complex oxide catalysts such as Fe-Al [12, 13], Fe-Al-Zn-Mg [14-19], and Fe-Co-Mg-Al [20-23] have high activity for the ODH of ethylbenzene. It is expected that these metal oxides can be applied to the ODH of 1-C_4H_8 as well.

In the present study, we aimed to develop catalysts that enable high performance for the ODH of 1-C_4H_8 using the lattice oxygen by adding metal oxides such as MgO, CoO, and ZnO to V-based complex oxides. In addition, given that the ODH of 1-C_4H_8 using molecular oxygen is required for the continuous production of BD, we examined whether these catalysts can maintain the activity of the ODH of 1-C_4H_8 under an O_2 atmosphere.

2. Experimental

2.1 Materials

NH_4VO_3 (assay = min. 99.0 %), $Co(NO_3)_2 \cdot 6H_2O$ (assay = min. 99.0 %), $Mg(NO_3)_2 \cdot 6H_2O$ (assay = min. 99.0 %), $Fe(NO_3)_3 \cdot 9H_2O$ (assay = min. 99.0 %), $Zn(NO_3)_2 \cdot 6H_2O$ (assay = min. 99.0 %), and citric acid (assay = min. 98.0 %) were purchased from Wako Pure Industries. But-1-ene (1-C_4H_8, assay = min. 99.0 %) was purchased from SUMITOMO SEIKA CHEMICALS CO., LTD.

2.2 Catalyst preparation by citric acid complex method

V-Mg(20:30), V-Mg-Fe(20:30:10), V-Mg-Zn(20:30:10), V-Mg-Co(20:30:1-30), V-Co(20:30), and V-Co-Mg(20:30:1-20) oxide catalysts were prepared according to the citric acid complex method. When these catalysts were prepared, NH_4VO_3 (1.17 g, 0.010 mol), $Mg(NO_3)_2 \cdot 6H_2O$ (3.85 g, 0.015 mol), and $Fe(NO_3)_3 \cdot 9H_2O$ (2.02 g, 0.005 mol), $Zn(NO_3)_2 \cdot 6H_2O$ (1.50 g, 0.005 mol), or $Co(NO_3)_2 \cdot 6H_2O$ (0.17-4.38 g, 0.0005-0.015 mol) were dissolved in 30 mL of the citric acid (4.80-7.68 g) aqueous solution. After standing for 24 h at a room temperature, the water was slowly evaporated from the mixed solution in an oil bath at 80℃. The catalysts were then calcined at 600℃ for 15 h in air.

2.3 Characterization of catalysts

In order to analyze the crystalline structure of the catalysts before and after the reaction, X-ray diffraction (XRD) analysis was carried out according to the powder method with a Shimadzu XRD-6000 diffraction meter with monochromatic CuKα radiation (tube voltage 40 kV, tube current 30 mA, scan step 0.02°, scan region 10-80°, scan rate 1.0°/min). X-ray photoelectron spectra (XPS) analysis was carried out with a Jeol model JPS-9010MX using MgKα radiation as the energy source. Surface areas of the catalysts were determined by the

BET method using N_2 adsorption equipment (Microtrac BEL, BELSORP-miniII-ISP). Samples were dried at 200℃ for 1 h prior to the measurement.

2.4 Catalyst test

2.4.1 ODH of 1-C_4H_8 with lattice oxygen

ODH of 1-C_4H_8 was carried out with a fixed-bed flow-type quartz reactor (10 mmϕ x 350 mm) at 480℃ under atmospheric pressure. Typical reaction conditions were as follows: after placing 200 mg of the catalyst in the reactor, the catalyst was heated to 480℃ under 25 mL/min of Ar. The reaction was carried out with 5 mL/min of 1-C_4H_8 and 25 mL/min of Ar for 0.5-8 min. The re-oxidation was carried out with 5 mL/min of O_2 and 25 mL/min of Ar at 480 ℃ for 8 min. The C_4 products (1-C_4H_8, *cis*-2-C_4H_8, *trans*-2-C_4H_8, and C_4H_6) were analyzed with a GC-FID (Shimadzu GC-14B, column: Unicarbon A-400). CO and CO_2 were also analyzed with a GC-FID (Shimadzu GC-14B, column: active carbon) equipped with a methanizer (Shimadzu MTN-1). H_2 was analyzed with a GC-TCD (Shimadzu GC-8A, column: active carbon).

2.4.2 ODH of 1-C_4H_8 under O_2 atmosphere

ODH of 1-C_4H_8 under an O_2 atmosphere was carried out with a fixed-bed flow-type quartz reactor (10 mmϕ x 350 mm) at 480℃ under atmospheric pressure. Typical reaction conditions were as follows: after placing 200 mg of the catalyst in the reactor, the catalyst was heated to 480℃ under 22.5 mL/min of Ar. The flow gas was switched to 5 mL/min of 1-C_4H_8, 22.5 mL/min of Ar, and 2.5 mL/min of O_2. The reactor was kept at 480℃ for 100 or 600 min. The C_4 products (1-C_4H_8, *cis*-2-C_4H_8, *trans*-2-C_4H_8, and C_4H_6), CO, and CO_2 were analyzed with a GC-FID as described in 2.4.1. H_2 was analyzed with a GC-TCD as described in 2.4.1.

3. Results and Discussion

3.1 Activity of V-Mg catalysts for ODH of 1-C_4H_8

3.1.1 Effect of adding metal oxides to V-Mg catalysts

Table 1 shows the results of 1-C_4H_8 ODH in the presence of V-Mg(20:30), V-Mg-Fe(20:30:10), V-Mg-Zn(20:30:10), and V-Mg-Co(20:30:10) catalysts with the lattice oxygen of the catalysts. The numerical values in parentheses indicate molar ratios. V-Mg(20:30) enabled high CO and CO_2 selectivity of 5.2 % and 10.2 %, respectively, and a low BD yield of 10.9 % (Run 1). When metal oxide-added V-Mg catalysts were used, CO and CO_2 selectivity were decreased to 1-4 % (Runs 2-4). V-Mg-Fe(20:30:10) enabled a high BD yield of 18.9 % (Run 2). V-Mg-Zn(20:30:10) resulted in a low BD yield of 12.9 % (Run 3) in contrast to other metal oxide-added V-Mg catalysts. The highest BD yield of 22.9 % was obtained with V-Mg-Co(20:30:10) (Run 4). V-Mg-Co(20:30:10) was the best catalyst for ODH using the lattice oxygen of the catalysts.

To clarify these results, we next measured the specific surface areas and XRD of the catalysts. Figure 1 illustrates the specific surface areas and the XRD patterns of V-Mg(20:30), V-Mg-Fe(20:30:10), V-Mg-Zn(20:30:10), and V-Mg-Co(20:30:10). The specific surface area of V-Mg (20:30) is smaller than those of other catalysts at 18 m^2/g. V-Mg-Zn(20:30:10) has a specific surface area of 19 m^2/g, and those of V-Mg-Fe(20:30:10) and V-Mg-Co(20:30:10) are nearly the same at 27 m^2/g and 26 m^2/g, respectively. These results suggest that among these

catalysts, those with large specific surface areas exhibit relatively high activity. Yet while this rule appear to be generally true, we noted that V-Mg-Co(20:30:10) enabled a higher BD yield than V-Mg-Fe(20:30:10) did. To explore this phenomenon, we next examined the crystalline structures of the catalysts.

V-Mg(20:30) and V-Mg-Fe(20:30:10) have the crystalline structure of $Mg_3V_2O_8$ only. The crystalline structures of $Mg_3V_2O_8$ and $Zn_3V_2O_8$ can be seen within V-Mg-Zn(20:30:10). It has been reported that the crystalline structure of $Mg_3V_2O_8$ contributes to ODH [10]. Therefore, V-Mg-Zn(20:30:10) has low activity for the ODH of 1-C_4H_8 because the crystalline structure of $Mg_3V_2O_8$ does not grow. V-Mg-Co(20:30:10) exhibits not only the diffraction peaks of $Mg_3V_2O_8$ but also those of $Mg_2V_2O_7$, Co_3O_4, and $Co_3V_2O_8$, which do not exist in V-Mg-Fe (20:30:10). It appears that the difference in ODH activity between V-Mg-Fe(20:30:10) and V-Mg-Co(20:30:10) is due to the crystalline structures of $Mg_2V_2O_7$, Co_3O_4, or $Co_3V_2O_8$. In other words, the crystalline structures of $Mg_2V_2O_7$, Co_3O_4, or $Co_3V_2O_8$ seem to contribute significantly to BD production in the ODH of 1-C_4H_8.

Table 1. Effect of metal (Fe, Zn, and Co) oxides addition to V-Mg catalysts for the ODH of 1-C_4H_8 with lattice oxygen of catalysts

Run	Catalyst	1-C_4H_8	Selectivity (%)					Yield (%)
		Conv. (%)	C_4H_6	*cis*-2-C_4H_8	*trans*-2-C_4H_8	CO	CO_2	C_4H_6
1	V-Mg(20:30)	33.3	40.0	23.8	20.9	5.2	10.2	10.9
2	V-Mg-Fe(20:30:10)	60.5	32.2	31.7	32.0	0.8	2.5	18.9
3	V-Mg-Zn(20:30:10)	61.7	23.3	35.3	36.2	1.0	3.1	12.9
4	V-Mg-Co(20:30:10)	60.7	39.7	28.9	27.5	0.5	3.4	22.9

Catalyst: 200 mg
Flow rate: 1-C_4H_8/Ar = 5(mL/min)/25(mL/min)
Reaction temp.: 480 ℃
Reaction time: 8 min

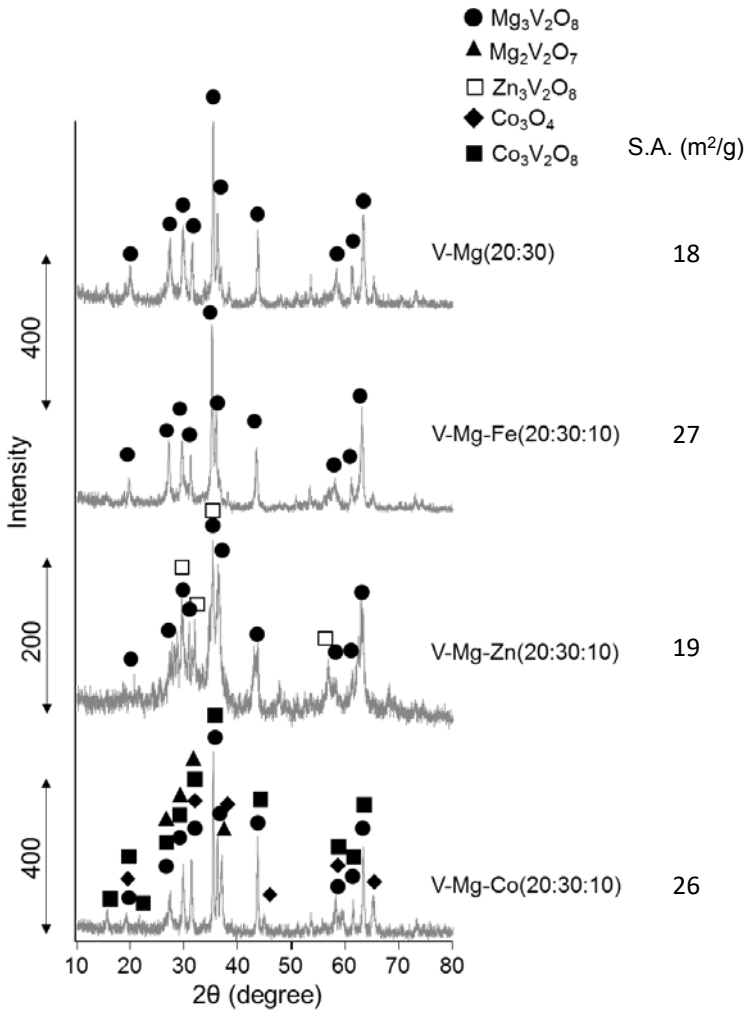

Figure 1. XRD patterns of V-Mg, V-Mg-Fe, V-Mg-Zn, and V-Mg-Co catalysts

3.1.2 Effects of different amounts of Co added to V-Mg-Co catalyst on ODH of 1-C_4H_8

In order to examine how different amounts of Co added to V-Mg-Co affect the ODH of 1-C_4H_8, V-Mg-Co catalysts were prepared with various Co content ratios. Table 2 shows the ODH of 1-C_4H_8 using V-Mg-Co catalysts with the lattice oxygen. V-Mg-Co(20:30:5) indicated the best activity, giving a high BD yield of 22.5 % and a low CO_2 selectivity of 3.2 %. As the Co content ratio increased, however, the BD selectivity and the BD yield significantly decreased.

We next investigated whether V-Mg-Co catalysts can maintain the activity of the ODH of 1-C_4H_8 under an O_2 atmosphere. Table 3 shows the ODH of 1-C_4H_8 using V-Mg and V-Mg-Co catalysts under an O_2 atmosphere. V-Mg-Co(20:30:5) exhibited excellent BD selectivity at 44.4 % and enabled a 1-C_4H_8 conversion of 25.2 % and a BD yield of 11.4 %. Contrary to the results shown in Table 2, the BD yield under an O_2 atmosphere increased as the Co ratio increased. V-Mg-Co(20:30:30) enabled the highest 1-C_4H_8 conversion of 33.0 % and a BD yield of 13.4 %.

To investigate the effects of differences in the crystallite structures of catalysts, we performed XRD analyses. Figure 2 shows the XRD patterns of V-Mg and V-Mg-Co catalysts. All of the catalysts have the crystalline structure of $Mg_3V_2O_8$. The diffraction peaks of $Mg_2V_2O_7$, $Co_3V_2O_8$, and Co_3O_4 were observed in V-Mg-Co(20:30:10, 20, 30) catalysts. The peak

intensities of $Co_3V_2O_8$ and Co_3O_4 were significantly higher in V-Mg-Co(20:30:20) and V-Mg-Co(20:30:30), indicating that Co_3O_4 and $Co_3V_2O_8$ contribute significantly more to the ODH of 1-C_4H_8 than $Mg_3V_2O_8$ does.

V-Mg-Co(20:30:5) exhibits high activity for the ODH of 1-C_4H_8 with the lattice oxygen but low activity for the same ODH process under an O_2 atmosphere. To explore the reasons for this, we conducted XRD analyses of V-Mg-Co(20:30:5) and V-Mg-Co(20:30:30) after the reaction. As shown in Figure 3, the crystalline structure of V-Mg-Co(20:30:5) changed from $Mg_3V_2O_8$ to MgO during the reaction, both with the lattice oxygen and under an O_2 atmosphere. In the XRD patterns of V-Mg-Co(20:30:30), the crystalline structure transformed to that of MgO and CoV_2O_4 during both reactions. It was expected that $Mg_3V_2O_8$ would yield high 1-C_4H_8 conversion and high BD selectivity in the early stage, but in practice, $Mg_3V_2O_8$ could not be maintained because the crystalline structure changed to that of MgO during the reactions. On the other hand, V-Mg-Co(20:30:30), which has the crystalline structures of $Co_3V_2O_8$ and CoV_2O_4, showed high activity for ODH under an O_2 atmosphere. Therefore, we cobluded that $Co_3V_2O_8$ and CoV_2O_4 have high activity for the ODH of 1-C_4H_8.

Table 2. Effect of Co addition amount on the ODH of 1-C_4H_8 with lattice oxygen of catalysts

Run	Catalyst	1-C_4H_8	Selectivity (%)					Yield (%)
		Conv. (%)	C_4H_6	*cis*-2-C_4H_8	*trans*-2-C_4H_8	CO	CO_2	C_4H_6
5	V-Mg-Co(20:30:5)	65.6	36.7	28.1	31.3	0.7	3.2	22.5
4	V-Mg-Co(20:30:10)	60.7	39.6	28.9	27.4	0.6	3.6	22.9
6	V-Mg-Co(20:30:20)	63.8	33.9	30.2	31.1	0.7	4.2	19.4
7	V-Mg-Co(20:30:30)	72.4	26.1	31.7	40.1	0.6	1.5	17.6

Catalyst: 200 mg
Flow rate: 1-C_4H_8/Ar = 5(mL/min)/25(mL/min)
Reaction temp.: 480 ℃
Reaction time: 8 min

Table 3. Effect of Co addition amount on the ODH of 1-C_4H_8 under O_2 atmosphere

Run	Catalyst	1-C_4H_8	Selectivity (%)					C_4H_6
		conv. (%)	C_4H_6	*cis*-2-C_4H_8	*trans*-2-C_4H_8	CO	CO_2	yield (%)
8	V-Mg(20:30)	32.9	22.5	25.9	22.1	7.7	21.8	7.4
9	V-Mg-Co(20:30:5)	25.2	44.4	16.0	12.3	4.3	22.9	11.4
10	V-Mg-Co(20:30:10)	27.2	44.0	15.3	11.7	5.0	24.0	12.2
11	V-Mg-Co(20:30:20)	28.5	41.4	17.8	13.7	3.6	23.5	12.5
12	V-Mg-Co(20:30:30)	33.0	41.2	21.1	17.3	3.1	17.3	13.4

Catalyst: 200 mg
Flow rate: 1-C_4H_8/O_2/Ar = 5(mL/min)/2.5(ml/min)/22.5(mL/min)
Reaction temp.: 480 ℃
Reaction time: 100 min

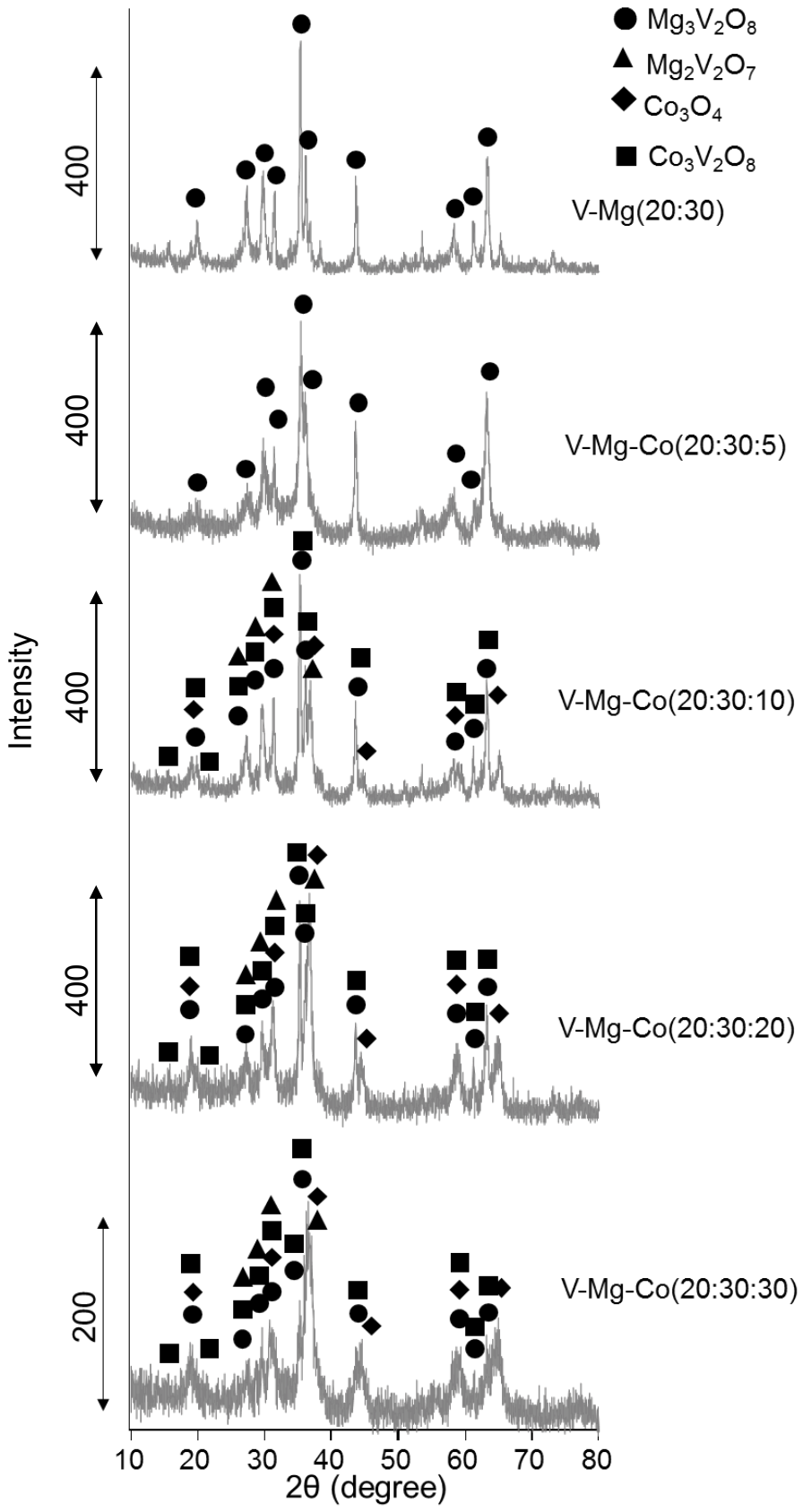

Figure 2. XRD patterns of V-Mg-Co catalysts

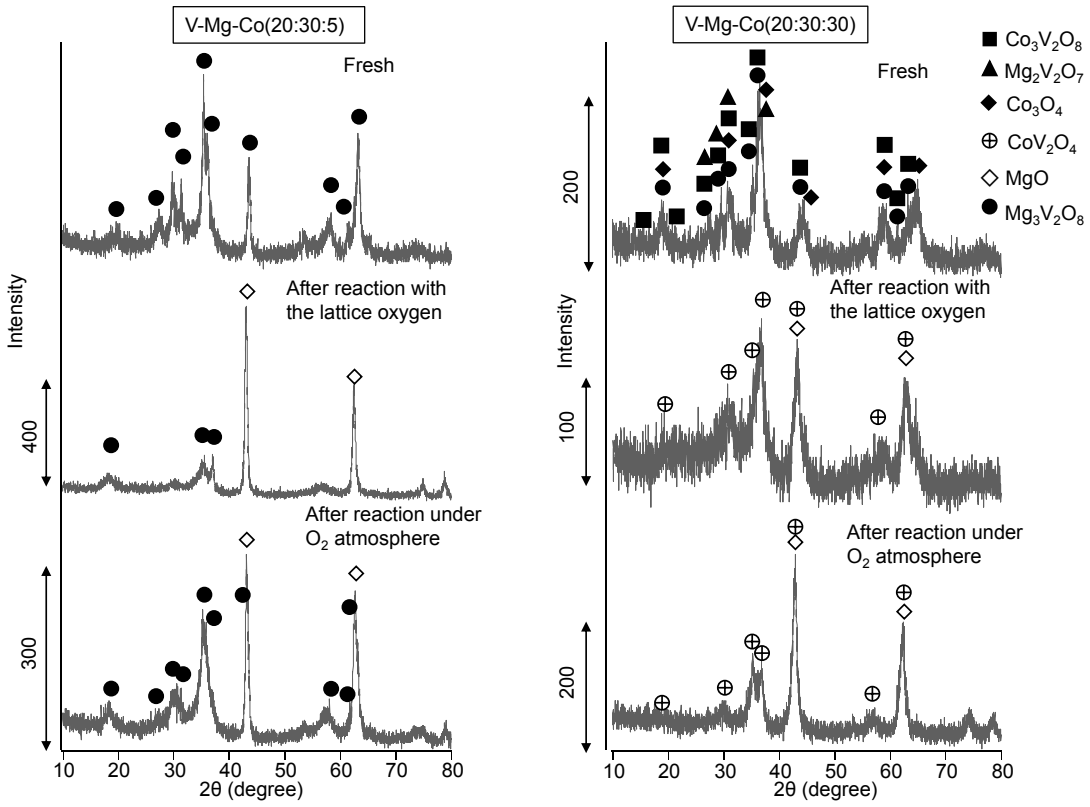

Figure 3. XRD patterns of V-Mg-Co(20:30:5) and V-Mg-Co(20:30:30) catalysts

3.2 Activity of V-Co catalysts for the ODH of 1-C_4H_8

3.2.1 Effect of various proportions of Mg added to V-Co-Mg catalyst

In order to examine whether $Co_3V_2O_8$ and CoV_2O_4 are capable of high activity for ODH, V-Co(20:30) was prepared. In addition, to investigate the possibility that the difference in the activity was related to the amount of Mg, V-Co-Mg(20:30:5-20) were prepared. The ODH of 1-C_4H_8 was conducted using these catalysts under an O_2 atmosphere. As shown in Table 4, V-Co(20:30) enabled a 1-C_4H_8 conversion of 38.2 % and a BD yield of 12.7 %. V-Co-Mg(20:30:5), in contrast, enabled a 1-C_4H_8 conversion of 31.8 % and a BD yield of 18.1 %. However, both the 1-C_4H_8 conversion and the BD yield decreased as the amount of added Mg decreased.

To interpret these results, we performed XRD analyses of the catalysts before and after the reactions. Figure 4 depicts XRD patterns of V-Co and V-Co-Mg catalysts before the reaction. All the catalysts have the crystalline structure of $Co_3V_2O_8$. When Mg was added, the diffraction peaks of $Mg_2V_2O_7$ and Co_3O_4 appeared. The intensity of these peaks increased as we increased the amount of Mg. Figure 5 shows the XRD patterns of V-Co and V-Co-Mg catalysts after the reactions. The crystalline structure of V-Co(20:30) changed to that of CoV_2O_4, and that of V-Co-Mg(20:30:5, 7.5, 10, 20) changed to that of CoV_2O_4 and MgO. The intensity of the diffraction peaks of MgO increased as we increased the amount of Mg. Both the 1-C_4H_8 conversion and the BD yield, however, decreased as the peak intensity of $Mg_2V_2O_7$ and MgO increased. It is known that $Mg_2V_2O_7$ yieldss higher 1-C_4H_8 conversion and lower BD

selectivity [11]. In addition, $Mg_2V_2O_7$ could not maintain its activity because of the difficulty of reoxidization [11]. Therefore, we concluded that adding excess of Mg decreases the activity of the ODH of 1-C_4H_8 to BD. Thus, V-Co-Mg(20:30:5) is the best catalyst for ODH under an O_2 atmosphere.

In order to investigate what makes V-Co-Mg(20:30:5) the best catalyst for ODH, we conducted XPS analyses of the catalysts. Figure 6 shows the XPS spectra of V-Co(20:30) and V-Co-Mg(20:30:5-20). Only V^{5+} was observed in these fresh catalysts. After the reactions, certain portions of this V^{5+} were reduced to V^{4+} and V^{3+}. After the reaction with V-Co(20:30), 30.6 % of the V^{5+}, which shows high activity for the ODH of 1-C_4H_8 [11], maintained in the catalyst. After the reaction with V-Co-Mg(20:30:5), which gave the highest activity, however, the percentage of V^{5+} remaining was the highest at 42.2 %. Figure 7 shows the relationship between the percentage of V^{5+} and the BD yield. The BD yield increased as the percentage of V^{5+} increased. V^{3+} is believed to exist mainly in bulk form, because our XRD analysis revealed that the crystalline structure of the catalyst after the reaction was that of CoV_2O_4. Yet the results of our XPS analysis revealed that V^{5+}, V^{4+}, and V^{3+} were present on the catalyst surface (Figure 6). These results indicate that the oxidation state of the V species of catalyst contributes to the BD production in the ODH of 1-C_4H_8. In addition, V-Co-Mg(20:30:5) showed high activity for ODH because the V species of the catalysts can maintain high oxidation states.

Table 4. Effect of Mg addition amount on the ODH of 1-C_4H_8 under O_2 atmosphere

Run	Catalyst	1-C_4H_8 conv. (%)	Selectivity (%)					C_4H_6 yield (%)
			C_4H_6	*cis*-2-C_4H_8	*trans*-2-C_4H_8	CO	CO_2	
13	V-Co(20:30)	38.2	33.2	22.3	19.4	4.0	21.1	12.7
14	V-Co-Mg(20:30:5)	31.8	55.1	13.9	10.4	2.6	18.0	18.1
15	V-Co-Mg(20:30:7.5)	31.3	53.5	12.8	9.3	2.4	22.0	17.2
16	V-Co-Mg(20:30:10)	29.2	53.3	12.8	9.5	2.3	22.0	15.6
17	V-Co-Mg(20:30:20)	27.3	51.9	13.1	9.8	2.5	22.6	14.3

Catalyst: 200 mg
Flow rate: 1-C_4H_8/O_2/Ar = 5(mL/min)/2.5(ml/min)/22.5(mL/min)
Reaction temp.: 480 ℃
Reaction time: 100 min

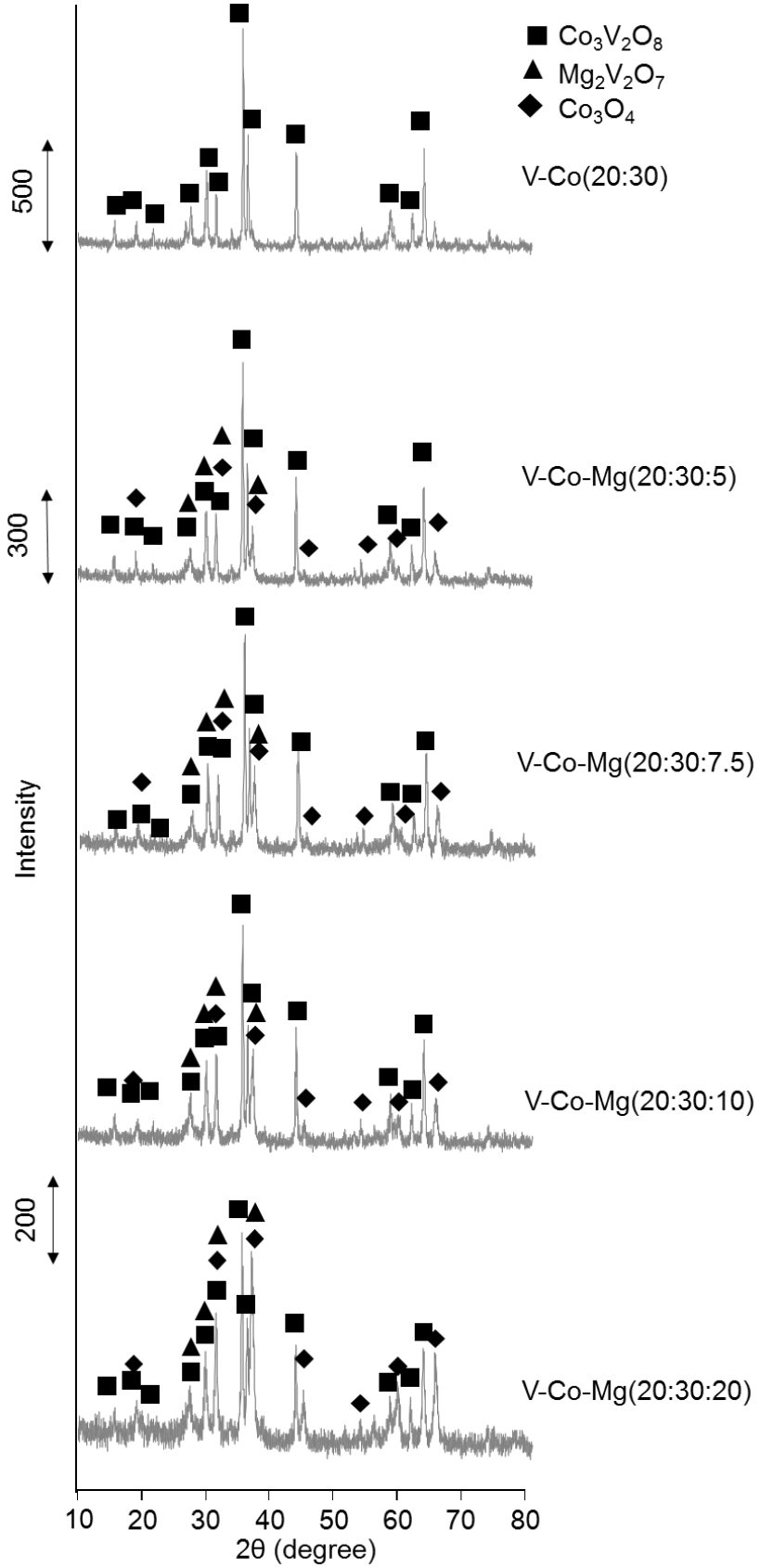

Figure 4. XRD patterns of V-Co-Mg catalysts

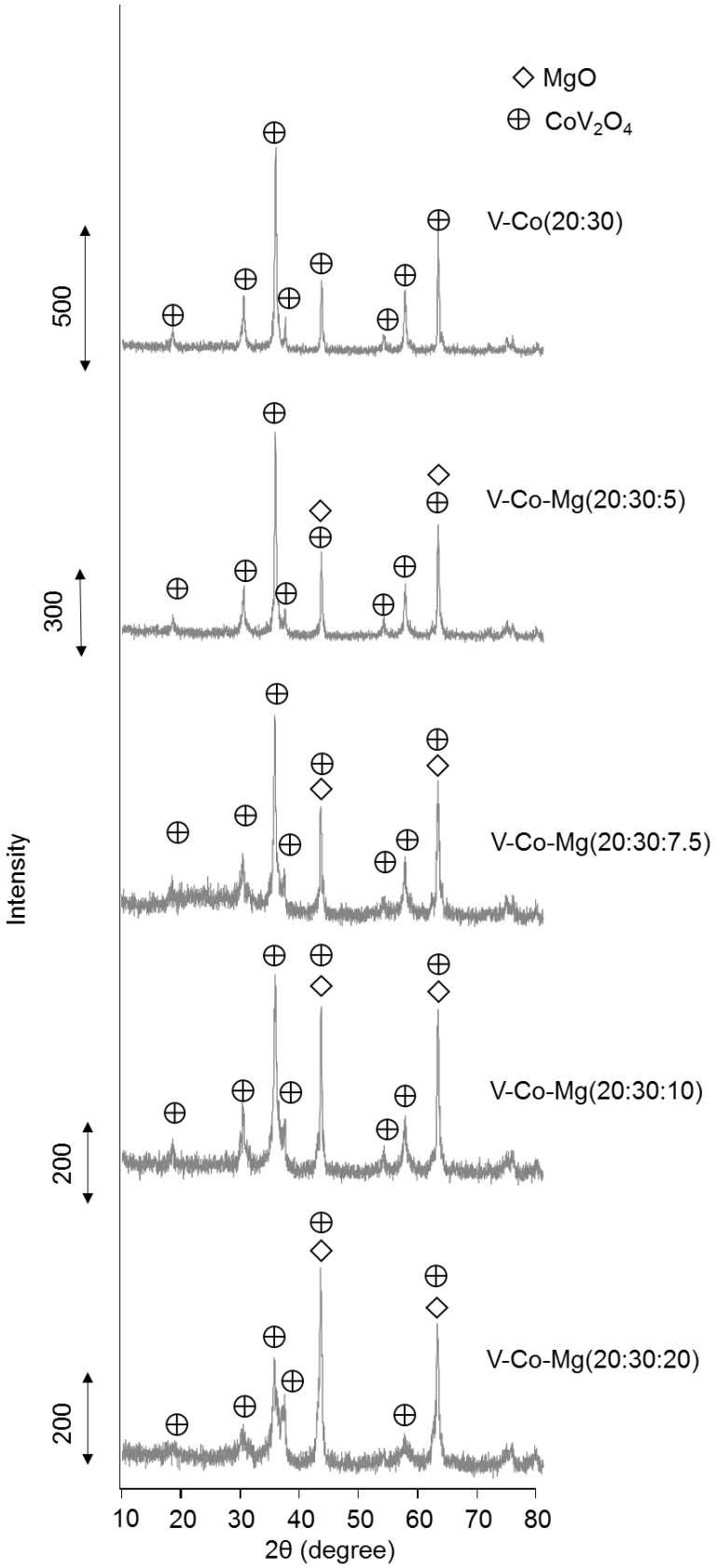

Figure 5. XRD patterns of V-Co-Mg catalysts (after 100 min reaction)

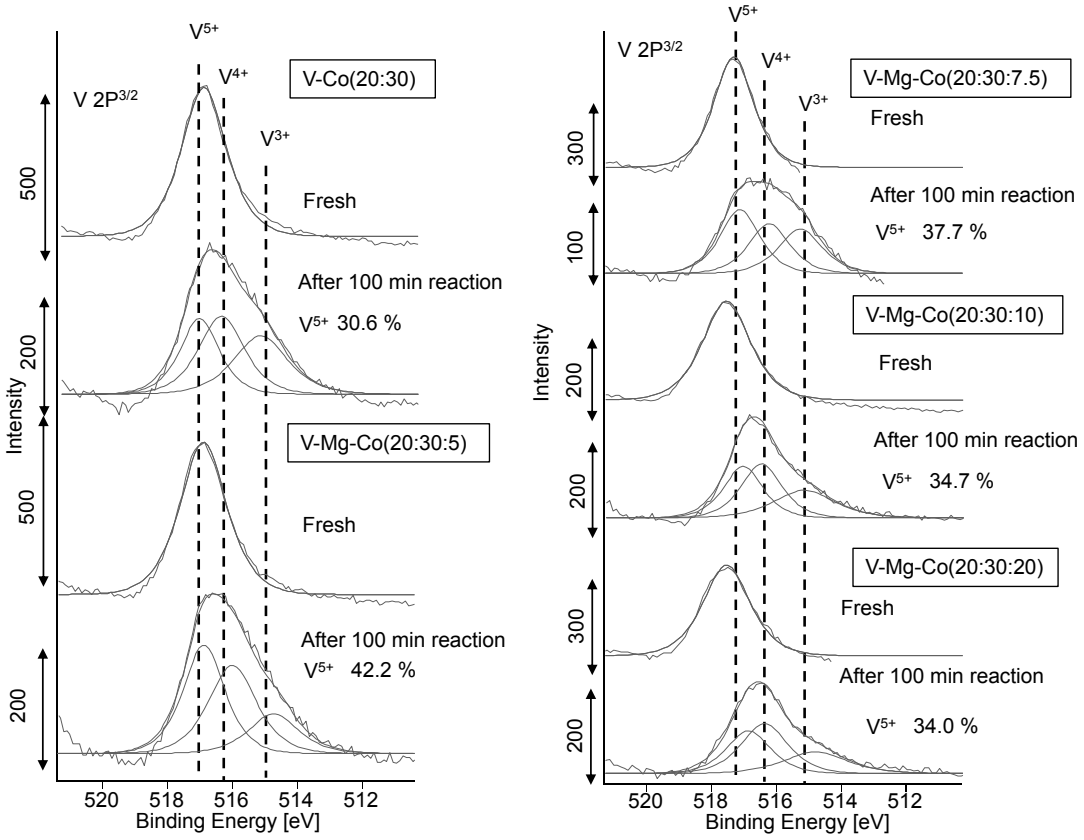

Figure 6. XPS spectra of V–Co–Mg catalysts

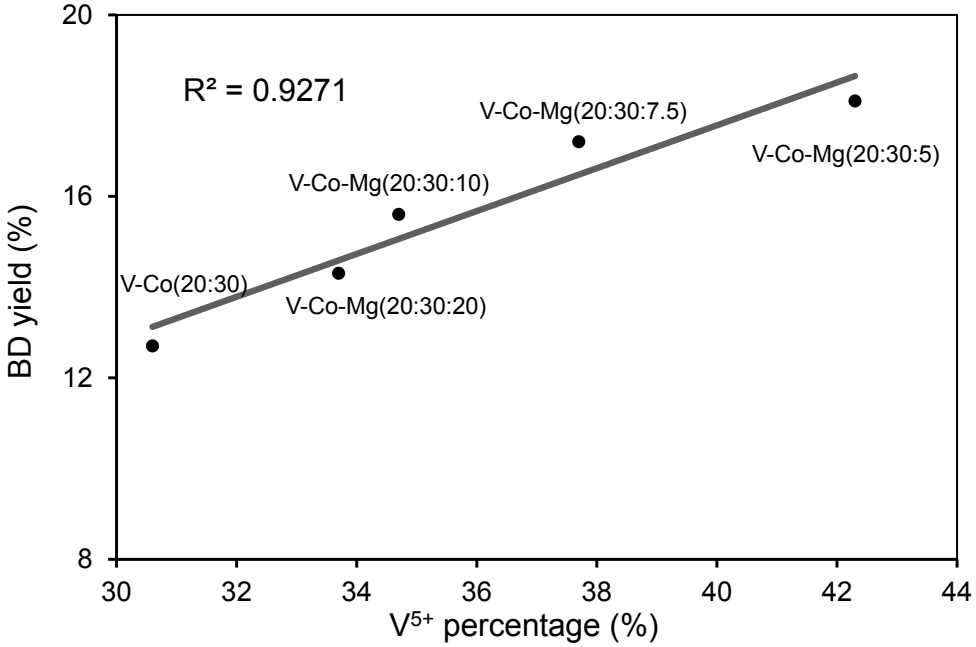

Figure 7. Relationship between the percentage of V^{5+} and the BD yield

3.2.2 Effect of reaction time on the ODH of 1-C_4H_8

The crystalline structure of V-Co-Mg(20:30:5) changed during a 100 min reaction (Figure 5); when this occurs. it is expected that the reactivity of this catalyst for ODH will change as well. To confirm this expectation, the effect of reaction time on the ODH of 1-C_4H_8 using the V-Co-Mg(20:30:5) catalyst under an O_2 atmosphere was examined. As shown in Figure 8 (Figure 8a: 0-20 min, Figure 8b: 20-600 min), the extremely high 1-C_4H_8 conversion of 66.1 % and a BD yield of 42.5 % were obtained during a 0.5-min reaction. As the reaction time increased up to 20 min, however, the 1-C_4H_8 conversion and the BD yield decreased. In particular, significant decreases in 1-C_4H_8 conversion and BD yield were observed between 0.5 min and 5 min. To explore the reasons for this, we conducted XRD analyses. Figure 9 shows the XRD patterns of V-Co-Mg(20:30:5) before and after the reactions. During the 5 min reaction, the crystalline structure changed completely from that of $Co_3V_2O_8$, $Mg_2V_2O_7$, and Co_3O_4 to that of CoV_2O_4 and MgO. It appears that this change in the crystalline structure of $Co_3V_2O_8$ is a cause of the significant decrease in activity over time. As the results in Figure 8a and Figure 9 reveal, the crystalline structure of $Co_3V_2O_8$ can exhibit excellent activity for the ODH of 1-C_4H_8, but the stability of $Co_3V_2O_8$ is low, resulting in a decreased activity over time.

Although the 1-C_4H_8 conversion decreased until 100 min (Figure 8b), the BD yield was maintained at 17.5 % throughout the 100 min reaction. The 1-C_4H_8 conversion was suppressed because the isomerization reaction of 1-C_4H_8 was decreased. The *cis*-2-C_4H_8/*trans*-2-C_4H_8 ratio in the reaction remained stable at 1.3 for 600 min. According to our XPS analysis, no metals such as V, Co, and Mg were present on the catalyst surface after the reaction. These results suggest that the surface of this catalyst was acidic [24]. It is known that the isomerization reaction of 1-C_4H_8 can be promoted by the acid sites of the catalyst [25]. During the 20 min reaction, the deposited carbon calculated from the TG analysis was 53.1 μmol (0.32 wt%). During the 100 min reaction, the deposited carbon increased to 169.1 μmol (1.01 wt%). The carbon was deposited on the acid sites of the catalyst during the ODH of 1-C_4H_8 under an O_2 atmosphere, decreasing its activity for isomerization. The BD selectivity, however, increased between 20 and 100 min. The 1-C_4H_8 conversion and the BD yield were maintained at 28.5 % and 17.5 %, respectively, even during a 600 min. reaction. During this 600 min reaction, notably, the crystalline structure of the catalyst remained as it was during the 100 min reaction (Figure 9). These results suggest that the crystalline structure of CoV_2O_4 can produce BD continuously in the ODH of 1-C_4H_8 under an O_2 atmosphere. In addition, to explore how V-Co-Mg(20:30:5) can maintain its activity for 600 min, we conducted XPS analyses of the catalyst after a 600 min reaction. Figure 10 shows the XPS spectra of V-Co-Mg(20:30:5). During the 600 min reaction, the percentage of V^{5+} was 42.3 %, which is almost identical to the percentage of V^{5+} in the catalyst used for ODH for 100 min (42.2 %). Thus V-Co-Mg(20:30:5) can maintain its activity because its percentage of V^{5+} stays constant whether the reaction lasts 100 or 600 min.

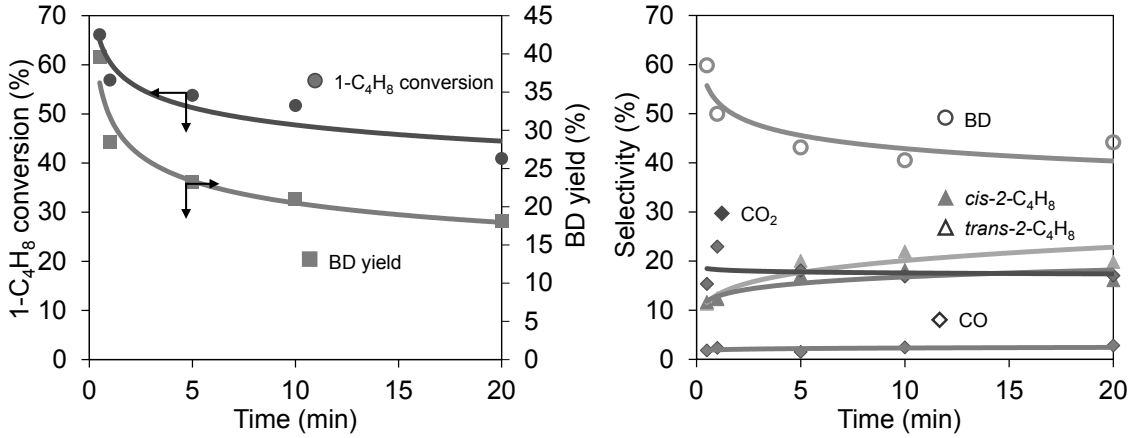

Catalyst: 200 mg, Flow rate: 30 mL/min (1-C_4H_8 /O_2/Ar = 5/2.5/22.5)
Reaction temp.: 480 °C

Figure 8a. Effect of reaction time on the ODH of 1-C_4H_8 with V-Co-Mg (20:30:5) catalyst (Reaction time: 0-20)

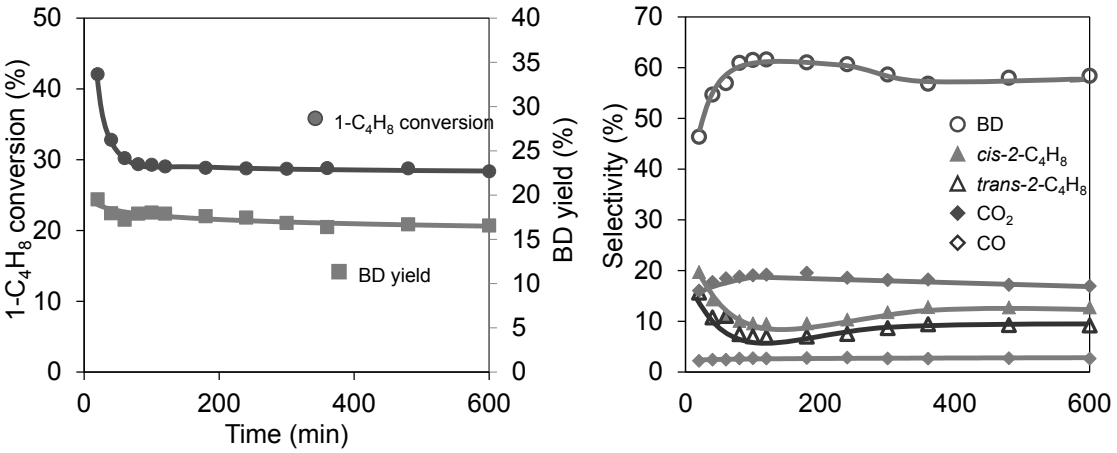

Catalyst: 200 mg, Flow rate: 30 mL/min (1-C_4H_8 /O_2/Ar = 5/2.5/22.5)
Reaction temp.: 480 °C

Figure 8b. Effect of reaction time on the ODH of 1-C_4H_8 with V-Co-Mg (20:30:5) catalyst (Reaction time: 20-600)

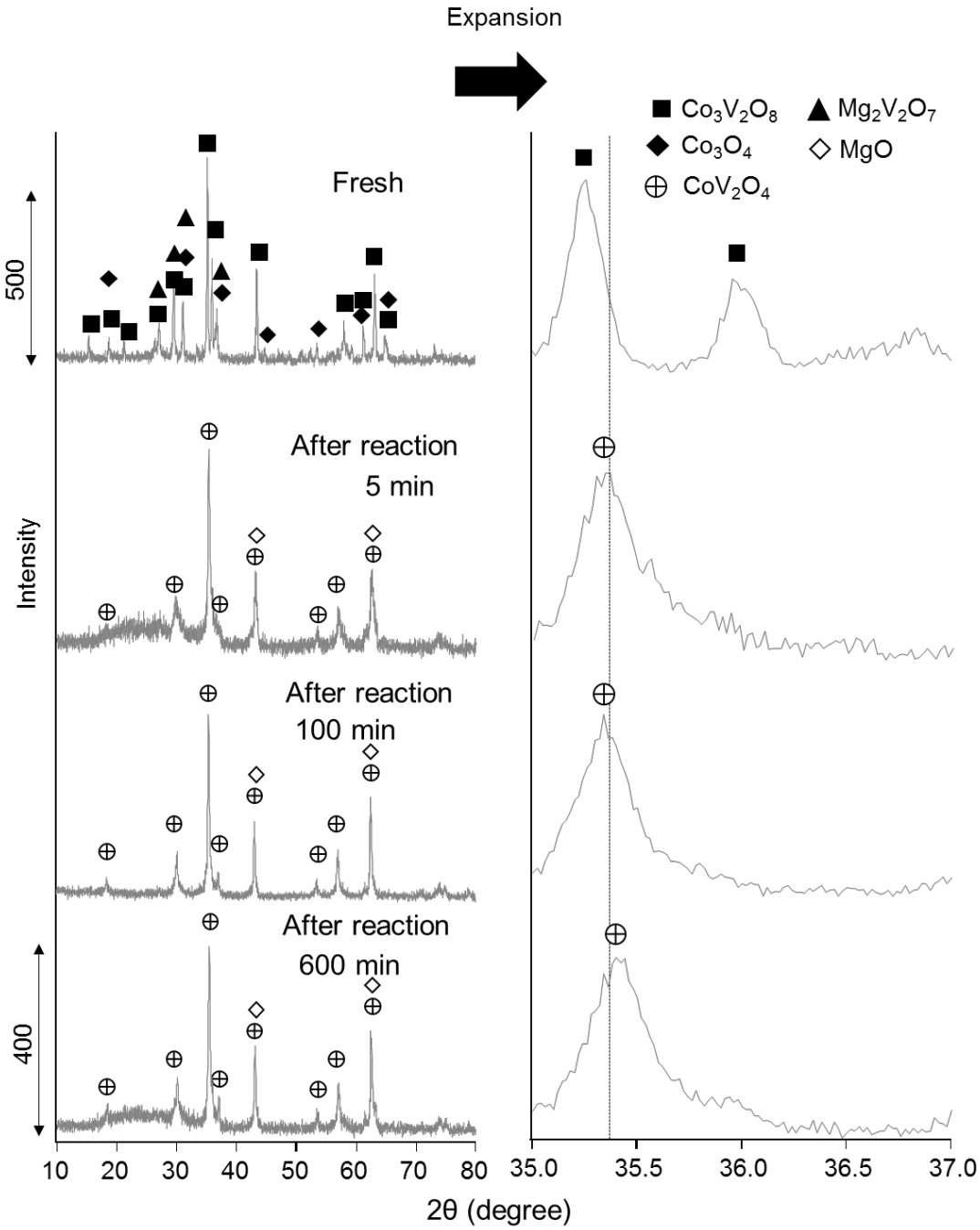

Figure 9. XRD patterns of V-Co-Mg(20:30:5) catalysts

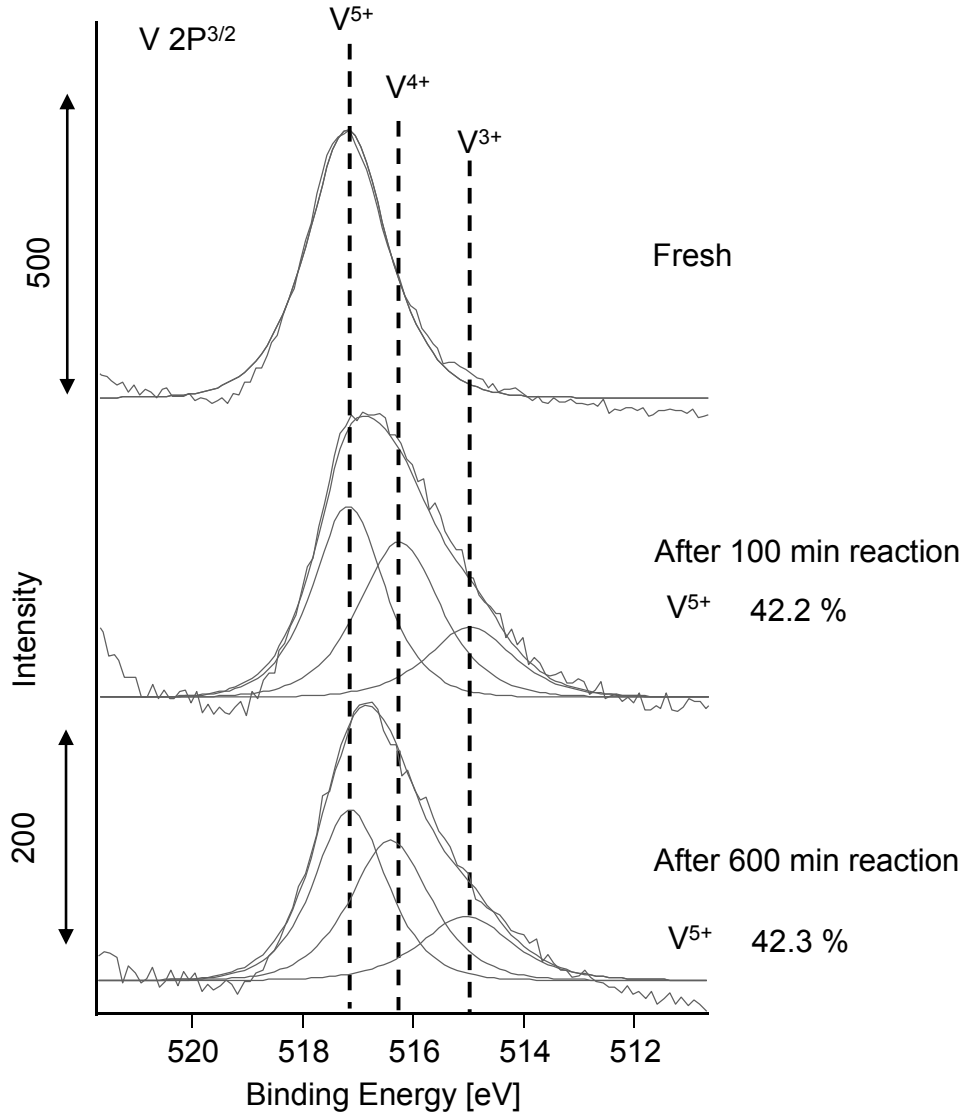

Figure 10. XPS spectra of V-Co-Mg(20:30:5) catalysts

3.2.3 Pulse reaction of 1-C_4H_8 and $^{18}O_2$

A pulse reaction of 1-C_4H_8 and $^{18}O_2$ was carried out to clarify the reaction mechanism of ODH on V-Co-Mg(20:30:5). As shown in Figure 11, at the moment when the pulse was sent, BD (m/z=54), CO_2 (m/z=44), and H_2O (m/z=18) were observed, but $H_2{}^{18}O$ (m/z=20) was not produced. Therefore, the fresh V-Co-Mg(20:30:5) catalyst could induce the ODH of 1-C_4H_8 using the lattice oxygen of the catalyst. The intensity of the $C^{18}O_2$ (m/z=48) peak increased as the number of pulses increased. Thus $^{18}O_2$ must be used for the oxidation of the deposited carbon or the re-oxidation of the catalyst, because $H_2{}^{18}O$ (m/z=20) was not observed. Therefore, the lattice oxygen of $Co_3V_2O_8$ might be used for the ODH of 1-C_4H_8 at the first stage of the reaction.

The pulse reaction was carried out with V-Co-Mg(20:30:5) that had been used in the ODH of 1-C_4H_8 under an O_2 atmosphere for 100 min. As shown in Figure 12, $^{18}O_2$ must have been used for the ODH of 1-C_4H_8 or the complete oxidation of the substrates, because BD (m/

z=54), $H_2{}^{18}O$ (m/z=20), and $C^{18}O_2$ (m/z=48) were produced. After the 100 min reaction, the crystalline structure of the catalyst was CoV_2O_4 as opposed to $Co_3V_2O_8$ (Figure 9). Therefore, we concluded that molecular O_2 was not used for the re-oxidation of the catalyst. Rather, molecular O_2 was assumed to absorb and react on the surface of the catalyst. To support this assumption, ODH using V-Co-Mg(20:30:5) that had been used in the ODH under an O_2 atmosphere for 100 min was carried out with the lattice oxygen. This reaction produced 136.4 μmol of BD, which is almost identical to the amount of produced H_2 (133.3 μmol). This result suggests that only the simple dehydrogenation of 1-C_4H_8 occurred. In other words, the lattice oxygen of CoV_2O_4 was not used for ODH under these conditions. It is likely, therefore, that ODH can proceed with the oxygen adsorbed on the surface of CoV_2O_4.

From these results, we concluded that the reaction mechanism is depicted in Scheme 1. In the first stage of the reaction, the ODH of 1-C_4H_8 progresses using the lattice oxygen of $Co_3V_2O_8$. During the production of BD, H_2O, and CO_2, $Co_3V_2O_8$ rapidly changes to CoV_2O_4 (Figure 9). At the next stage, the ODH reaction transfers to the catalyst cycle as shown in Scheme 1. A portion of the 1-C_4H_8 that was adsorbed on the catalyst is deposited as carbon on the surface of CoV_2O_4, then oxidized into CO_2 by molecular O_2 which had been adsorbed on the surface of CoV_2O_4. The ODH of 1-C_4H_8 can thus progress using the O_2 adsorbed on the catalyst surface. In the reaction cycle, it is likely that these reactions occur almost simultaneously, because BD (m/z=54), $H_2{}^{18}O$ (m/z=20), and $C^{18}O_2$ (m/z=48) were observed at the same time (Figure 12).

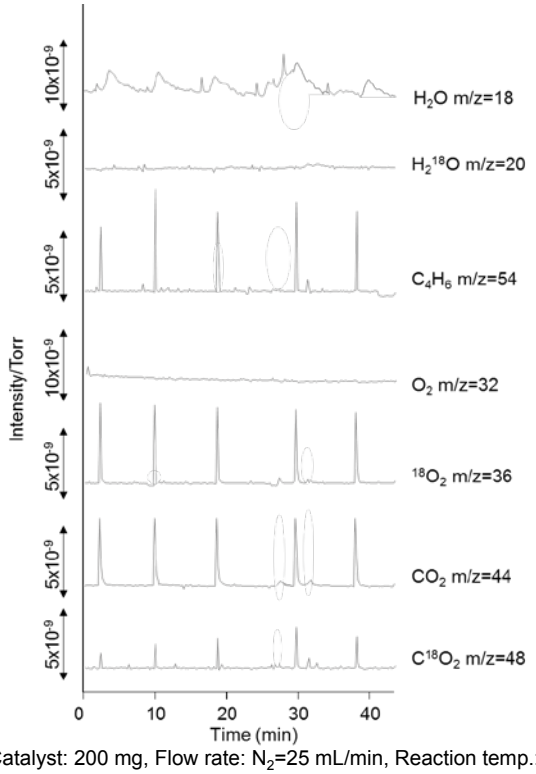

Catalyst: 200 mg, Flow rate: N_2=25 mL/min, Reaction temp.: 480 °C
Gas volume rate: 1-C_4H_8/$^{18}O_2$=2/1, Pulse: 1 mL

Figure 11. 1-C_4H_8 and $^{18}O_2$ pulse reaction profiles of V-Mg-Co(20:30:5) catalyst (fresh)

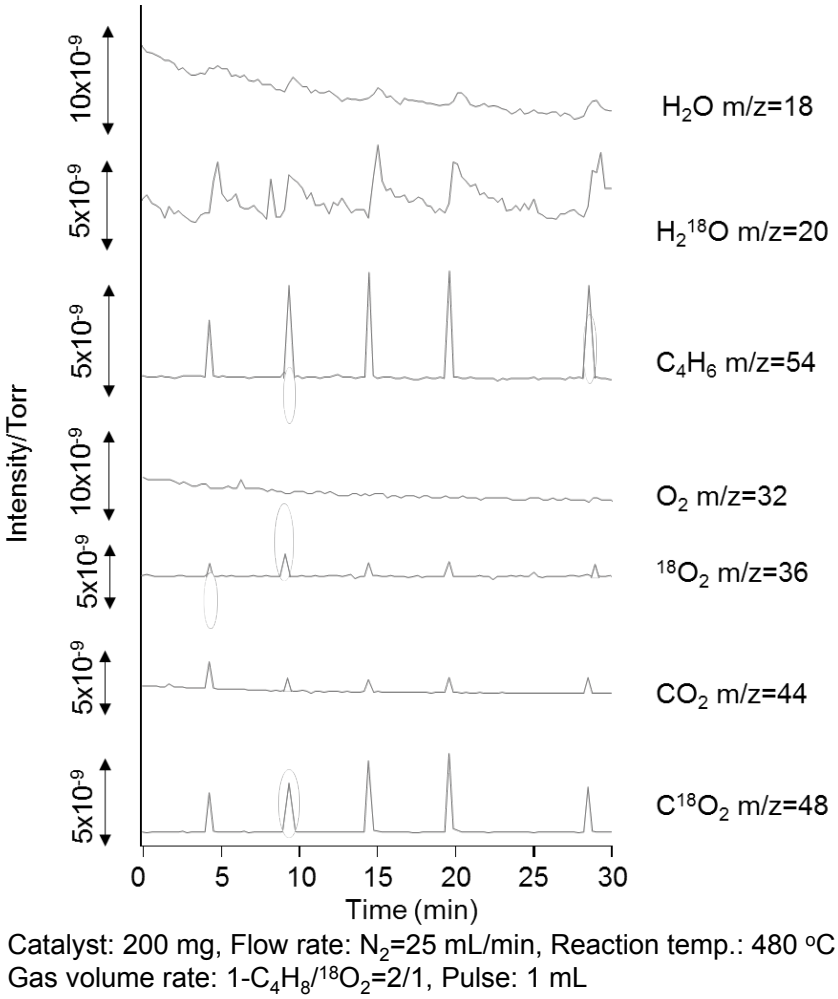

Figure 12. 1-C_4H_8 and $^{18}O_2$ pulse reaction profiles of V-Mg-Co(20:30:5) catalyst (after 100-min reaction)

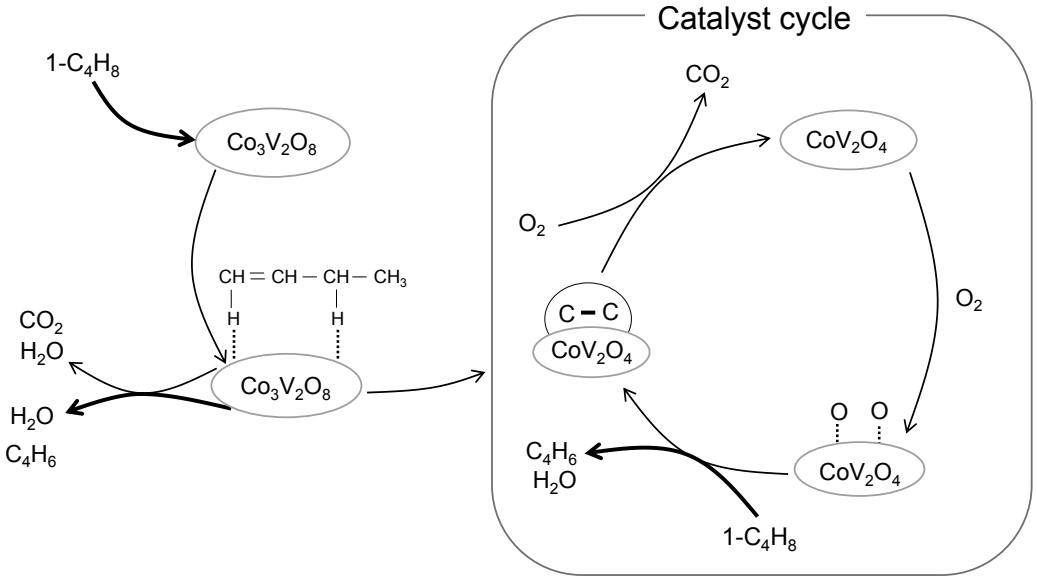

Scheme 1. Reaction mechanism for the ODH of 1-C_4H_8 under O_2 atmosphere with V-Co-Mg(20:30:5)

4. Conclusions

The V-Mg-Co(20:30:5) catalyst gave a high BD yield of 22.5 % in the ODH of 1-C_4H_8 with the lattice oxygen of the catalyst. The V-Co catalysts, which have the crystalline structure of $Co_3V_2O_4$ and CoV_2O_4, were more active than the V-Mg catalysts for ODH under an O_2 atmosphere. The V-Co-Mg(20:30:5) catalyst has the highest activity for the ODH of 1-C_4H_8 under an O_2 atmosphere, maintaining a 1-C_4H_8 conversion of 28.5 % and a BD yield of 17.5 % for 600 min. The percentage of V^{5+} on the surface of the catalyst affects the 1-C_4H_8 conversion and the BD yield. Preserving high valence of in the V species is important to maintain their capacity for ODH over the long term. It is likely that $Co_3V_2O_8$ is highly active in the early stage of ODH, whereas in the later stages, ODH proceeds using oxygen adsorbed on the surface of CoV_2O_4.

References

[1] K. Fujimoto, *J. Soc. Rubber Sci. Technol.* **34**, 532-537 (1961).

[2] J. C. Jung, H. Kim, Y. S. Kim, Y-M. Chung, T. J. Kim, S. J. Lee, S-H. Oh, I. K. Song, *Appl. Catal. A*, **317**, 244-249 (2007).

[3] J. C. Jung, H. Lee, H. Kim, Y-M. Chung, T. J. Kim, S. J. Lee, S-H. Oh, Y. S. Kim, I. K. Song, *Catal. Commun.*, **9**, 447-452 (2008).

[4] A. P. V. Soares, L. D. Dimitrov, M. C-R. A. Oliveira, L. Hilaire, M. F. Portela, R. K. Grasselli, *Appl. Catal. A*, **253**, 191-200 (2003).

[5] H. Lee, J. C. Jung, H. Kim, Y-M. Chung, T. J. Kim, S. J. Lee, S. H. Oh, Y. S. Kim, I. K. Song, *Catal. Commun.*, **9**, 1137-1142 (2008).

[6] J. A. Toledo-Antonio, N. Nava, M. Martínez, X. Bokhimi, *Appl. Catal. A*, **234**, 137-144 (2002).

[7] H. Lee, J. C. Jung, I. K. Song, *Catal. Lett.*, **133**, 321-327 (2009).

[8] M. Shimamura, F. Nozaki, *Nipppon Kagaku Kaishi*, **12**, 1879-1884 (1982).

[9] K. Fukudome, N. Ikenaga, T. Miyake, T. Suzuki, *Catal. Sci. Technol.*, **1**, 987-998 (2011).

[10] T. Kiyokawa, T. Hagihara, N. Ikenaga, *ChemistrySelect*, **4**, 906-913 (2019).

[11] Y. Sakurai, T. Suzaki, N. Ikenaga, H. Aota, T. Suzuki, *Chem. Lett.*, **5**, 526-527 (2000).

[12] N. Mimura, I. Takahara, M. Saito, T. Hattori, K. Ohkuma, M. Ando, *Catal. Today*, **45**, 61-64 (1998).

[13] N. Mimura, M. Saito, *Catal. Today*, **55**, 173-178 (2000).

[14] N. Mimura, I. Takahara, M. Saito, Y. Sasaki, K. Murata, *Catal. Lett.*, **78**, 125-128 (2002).

[15] X. Ye, N. Mac, W. Hua, Y. Yue, C. Miao, Z. Xie, Z. Gao, *J. Mol. Catal. A: Chem.*, **217**, 103-108 (2004).

[16] A. Sun, Z. Qin, S. Chen, *J. Wan, J. Mol. Catal. A: Chem.*, **210**, 189-195 (2004).

[17] P. Kustrowski, A. Rafalska-Lasocha, D. Majda, D. Tomaszewska, R. Dziembaj, *Solid State Ionics*, **141-142**, 237-242 (2001).

[18] M. Ji, G. Chen, J. Wang, X. Wang, T. Zhang, *Catal. Today*, **158**, 464-469 (2010).

[19] Y. Ohishi, T. Kawabata, T. Shishido, K. Takaki, Q. Zhang, Y. Wang, K. Nomura, K. Takehira, *Appl. Catal. A*, **288**, 220-231 (2005).

[20] R. J. Balasamy, A. Khurshid, A A. S. Al-Ali, L. A. Atanda, K. Sagata, M. Asamoto, H. Yahiro, K.

Nomura, T. Sano, K. Takehira, S. S. Al-Khattaf, *Appl. Catal. A*, **398**, 113-122 (2011).

[21] L. A. Atanda, R. J. Balasamy, A. Khurshid, A. A. S. Al-Ali, K. Sagata, M. Asamoto, H. Yahiro, K. Nomura, T. Sano, K. Takehira, S. S. Al-Khattaf, *Appl. Catal. A*, **396**, 107-115 (2011).

[22] B. B. Tope, R. J. Balasamy, A. Khurshid, L. A. Atanda, H. Yahiro, T. Shiono, K. Takehira, S. S. Al-Khattaf, *Appl. Catal. A*, **407**, 118-126 (2011).

[23] R. J. Balasamy, A. Khurshid, A. A. S. Al-Ali, L. A. Atanda, K. Sagata, M. Asamoto, H. Yahiro, K. Nomura, T. Sano, K. Takehira, S. S. Al-Khattaf, *Appl. Catal. A*, **390**, 225-234 (2010).

[24] E. Kikuchi, K. Segawa, A. Tada, H. Hattori, Y. Imizu, "New Catalytic Chemistry", Sankyo Publishing, **2**, 233-234 (1997).

[25] A. Beres, I. Hannus, I. Kiricsi, R. Kinet., *Catal. Lett.*, **56**, 55-61 (1995).